

The Endosomal Na^+/H^+ Exchanger Contributes to Multivesicular Body Formation by Regulating the Recruitment of ESCRT-0 Vps27p to the Endosomal Membrane^{*[S]}

Received for publication, May 12, 2011, and in revised form, August 11, 2011 Published, JBC Papers in Press, September 5, 2011, DOI 10.1074/jbc.M111.260612

Keiji Mitsui¹, Yuri Koshimura, Yuriko Yoshikawa, Masafumi Matsushita, and Hiroshi Kanazawa²

From the Department of Biological Sciences, Graduate School of Science, Osaka University, Machikaneyama-cho 1-1, Toyonaka City, Osaka, Japan 560-0043

Multivesicular bodies (MVBs) are late endosomal compartments containing luminal vesicles (MVB vesicles) that are formed by inward budding of the endosomal membrane. In budding yeast, MVBs are an important cellular mechanism for the transport of membrane proteins to the vacuolar lumen. This process requires a class E subset of vacuolar protein sorting (VPS) genes. *VPS44* (allelic to *NHX1*) encodes an endosome-localized Na^+/H^+ exchanger. The function of the *VPS44* exchanger in the context of vacuolar protein transport is largely unknown. Using a cell-free MVB formation assay system, we demonstrated that Nhxl1p is required for the efficient formation of MVB vesicles in the late endosome. The recruitment of Vps27p, a class E Vps protein, to the endosomal membrane was dependent on Nhxl1p activity and was enhanced by an acidic pH at the endosomal surface. Taken together, we propose that Nhxl1p contributes to MVB formation by the recruitment of Vps27p to the endosomal membrane, possibly through Nhxl1p antiporter activity.

Multivesicular bodies (MVBs)³ are a subset of late endosomes that contain internal vesicles, permitting precursor and plasma membrane proteins to reach the lysosome or vacuole lumen for degradation or maturation, respectively. In eukaryotic cells, the MVB pathway controls various important processes such as receptor down-regulation, antigen presentation, cytokinesis, retroviral budding, and autophagy (1–6). In the budding yeast *Saccharomyces cerevisiae*, previous studies identified a number of genes involved in vacuolar protein sorting (VPS) (7, 8). These Vps proteins function at distinct steps of protein transport between the Golgi complex and the vacuole

(7, 8). A subset of Vps proteins, class E proteins, is involved in MVB formation. Most class E proteins are components of five distinct complexes; Vps27p-Hse1p (also called endosomal sorting complexes required for transport-0 (ESCRT-0), -I, -II, and -III and Vps4p. These complexes are required for the formation of internal vesicles and sorting of cargo proteins to the vesicles from the endosomal membrane (3, 9). Vps27p (ESCRT-0) recruits ESCRT-I, which in turn recruits and/or activates ESCRT-II and ESCRT-III at the endosome (3, 10). Recent *in vitro* studies have provided new insights into the precise role of each ESCRT complex in MVB formation (11–13). ESCRT-0 initiates the MVB sorting process by recruiting ESCRT-I to the endosomal membrane and concentrating ubiquitylated MVB cargos to the vesicle budding site (12). ESCRT-I and ESCRT-II are directly involved in membrane budding by stabilizing the bud necks, whereas ESCRT-III is responsible for the cleavage of bud necks (11–13). Finally, the AAA-type ATPase Vps4p dissociates the ESCRT-III complex from the endosome (14). The sequential activity of these complexes on the cytoplasmic surface of endosomes directs the budding and fission of vesicles into the lumen of the endosome and the sequestration of cargo proteins in the vesicle. Defects in ESCRT proteins prevent internal vesicle formation and result in exaggerated class E compartments (9, 15).

Na^+/H^+ exchangers (NHEs) are ubiquitous membrane proteins found in various species from yeast to humans and higher plants (16). NHEs exchange sodium (or potassium) for protons across the membranes and play an important physiological role in the regulation of intracellular pH and sodium ion concentration (17–22). Although NHE1–5 are mainly found in plasma membranes, NHE6–9 are mainly distributed to organellar membranes. We have shown previously that in mammalian cells Na^+/H^+ exchangers contribute to endosomal pH homeostasis by allowing proton leakage from the endosomal lumen in cooperation with V-ATPase activity (23–26). The budding yeast *S. cerevisiae* also expresses Na^+/H^+ exchangers, one of which, Nhxl1p, localizes to the late endosomes (prevacuolar compartment) and is highly homologous to the NHEs found in mammalian cells (27, 28). When grown in medium with extremely low pH (<4.0), *NHX1*-disrupted (*nhx1Δ*) cells show defects in cell growth and excess acidification of the vacuolar lumen compared with wild-type cells (28, 29), suggesting that Nhxl1p also contributes to pH homeostasis of organelles. In

* This work was supported by a grant-in-aid from the Japanese Ministry of Education, Science, Sports, Technology, and Culture.

[S] The on-line version of this article (available at <http://www.jbc.org>) contains supplemental Table S1 and Figs. S1–S3.

¹ To whom correspondence may be addressed. E-mail: mitsui8@bio.sci.osaka-u.ac.jp.

² To whom correspondence may be addressed. Tel.: 81-6-6850-5812; Fax: 81-6-6850-5812; E-mail: kanazawa@bio.sci.osaka-u.ac.jp.

³ The abbreviations used are: MVB, multivesicular body; DPX, *p*-xylene-bispyridinium bromide; ESCRT, endosomal sorting complexes required for transport; HPTS, 8-hydroxypyrene-1,3,6-trisulfonate; NHE, Na^+/H^+ exchanger; VPS, vacuolar protein sorting; PI(3)P, phosphatidylinositol 3-phosphate; DIC, differential interference contrast; t-SNARE, target soluble *N*-ethylmaleimide factor attachment protein receptor; EGFP, enhanced green fluorescent protein; TAP, tandem affinity purification.

TABLE 1

Yeast strains used in this study

Strains	Genotype	Reference
BY4742	MAT α <i>his3Δ1 leu2Δ0 lys2Δ0 ura3Δ0</i>	Ref. 31
W303-1B	MAT α <i>ade2-1 his3-11,15 leu3112 trp1-1 ura3-1,60 can1-100</i>	Ref. 32
MKY0804	MAT α <i>his3Δ1 leu2Δ0 lys2Δ0 ura3Δ0 nhx1Δ::his5</i>	This study
MKY0614	MAT α <i>ade2-1 his3-11,15 leu3112 trp1-1 ura3-1,60 can1-100 nhx1Δ::LEU2</i>	Ref. 28
MKY0806	MAT α <i>his3Δ1 leu2Δ0 lys2Δ0 ura3Δ0 vps27Δ::his5</i>	This study
MKY1001	MAT α <i>his3Δ1 leu2Δ0 lys2Δ0 ura3Δ0 snf7Δ::his5</i>	This study
VPS27-TAP	MAT α <i>his3Δ1 leu2Δ0 met15Δ0 ura3Δ0 VPS27-TAP::HIS3MX6</i>	Open Biosystems
SNF7-TAP	MAT α <i>his3Δ1 leu2Δ0 met15Δ0 ura3Δ0 SNF7-TAP::HIS3MX6</i>	Open Biosystems
YYY01	MAT α <i>his3Δ1 leu2Δ0 met15Δ0 ura3Δ0 VPS27-TAP::HIS3MX6 nhx1Δ::LEU2</i>	This study
YYY02	MAT α <i>his3Δ1 leu2Δ0 met15Δ0 ura3Δ0 SNF7-TAP::HIS3MX vps27Δ::LEU2</i>	This study

addition, loss of *NHX1* causes a *VPS* phenotype that is characterized by the missorting of vacuolar carboxypeptidase Y to the extracellular space, improper transport of vacuolar proteins, and enlargement of the late endosomes (class E compartment) (29, 30). Accordingly, the *NHX1* gene is allelic to *VPS44*, which was classified as belonging to the class E *VPS* genes (30).

Although the precise role of each ESCRT complex, including class E proteins, in internal vesicle formation, fission, and cargo sorting of MVB has been studied extensively (11–13), there is no direct evidence that Nhx1p contributes to MVB formation. Furthermore, the potential role of pH in MVB formation has not been considered thus far. Here, we established an *in vitro* assay system to analyze MVB formation and demonstrated that Nhx1p contributes directly to MVB formation. Moreover, we showed that Nhx1p is required for endosomal recruitment of ESCRT proteins. Our results suggest a functional relationship between Nhx1p activity and MVB formation.

EXPERIMENTAL PROCEDURES

Strains, Media, and Growth Conditions—*S. cerevisiae* strains used in this study were derived from BY4742 (31) or W303-1B (32) strains and are listed in Table 1.

Standard yeast culture and genetic manipulations were performed as described by Sherman *et al.* (33). Transformation of yeast cells was performed by the lithium acetate method (33). All yeast strains were routinely cultured at 30 °C in YPAD medium (1% yeast extract, 2% peptone, 40 mg/liter adenine, and 2% glucose), SD medium (0.17% yeast nitrogen base without ammonium sulfate and amino acids, 0.5% ammonium sulfate, and 2% glucose) supplemented with the appropriate nucleotides and amino acids, or APG medium (10 mM arginine, 8 mM phosphoric acid, 2 mM MgSO₄, 1 mM KCl, 0.2 mM CaCl₂, 2% glucose, and trace minerals and vitamins) (34). The pH of the APG medium was adjusted to 5.5 by the addition of phosphoric acid. The *Escherichia coli* strain JM109 was used to propagate the plasmids. *E. coli* cells were cultured in L broth with an antibiotic appropriate for the selection of transformants, as described previously (35).

Yeast Lysate and Membrane Preparation—Yeast cells were grown at 30 °C in YPAD medium to early log phase, harvested, washed with distilled water and Tris sulfate-DTT buffer (100 mM Tris sulfate (pH 9.4), and 10 mM DTT), and then suspended in spheroplast buffer (1.0 M sorbitol and 0.75× yeast extract/peptone/dextrose medium). The cells were converted to spheroplasts by the addition of zymolyase and incubated for 30 min at 30 °C with gentle shaking. The resulting spheroplasts were collected by centrifugation through a cushion of 1.4 M

sorbitol and suspended in reaction buffer A (0.4 M sorbitol, 20 mM HEPES, 150 mM KCl, 1 mM DTT, and 5 mM magnesium acetate, pH adjusted to 7.2 with KOH) containing 1 mM phenylmethylsulfonyl fluoride (PMSF), 1 μ g/ml leupeptin, 1 μ g/ml pepstatin, and 1 μ g/ml aprotinin. The cells were homogenized on ice by 10 passes through a 26-gauge needle with a 1-ml syringe and then centrifuged twice at 400 × *g* for 5 min at 4 °C. The resulting supernatant was used as yeast lysate, which was further centrifuged at 13,000 × *g* for 15 min at 4 °C to obtain the endosome-rich membrane. The resulting pellet (P13 membrane) was resuspended in reaction buffer A at a final protein concentration of 5 mg/ml.

Yeast Cytosol Preparation—Yeast cells were grown at 30 °C in YPAD, harvested, resuspended in reaction buffer A supplemented with protease inhibitors, and ground in a mortar using liquid nitrogen. The lysate was centrifuged at 10,000 × *g* for 10 min and 100,000 × *g* for 1 h to sediment membranes. The supernatants were stored at −80 °C.

In Vitro Assay for MVB Formation—A 270- μ l aliquot of yeast lysate (5 mg/ml) was mixed on ice with 100 mM 8-hydroxypyrene-1,3,6-trisulfonate (HPTS) (Invitrogen, Molecular Probes) (3 μ l) and ATP-regenerating solution (30 μ l). The ATP-regenerating solution consisted of 10 mM ATP-potassium salt (Sigma), 400 mM phosphocreatine (Nacalai Tesque), and 100 units/ml creatine phosphokinase (Nacalai Tesque). This mixture was incubated at 30 °C for the indicated times. For assays using endosome-rich membranes, 50 μ l of P13 membrane (5 mg/ml) was incubated with 220 μ l of BSA (5 mg/ml) or cytosol (5 mg/ml) in the presence of 1 mM HPTS and ATP-regenerating solution at 30 °C for 30 min. To test the pH dependence of MVB formation, yeast lysates were prepared in reaction buffer B (0.4 M sorbitol, 50 mM MES, 50 mM HEPES, 75 mM KCl, 75 mM NaCl, 200 mM ammonium acetate, 10 mM NaN₃, 10 mM 2-deoxy-D-glucose, pH adjusted to 6.0 or 7.0 with acetic acid or KOH, respectively) containing 1 mM PMSF, 1 μ g/ml leupeptin, 1 μ g/ml pepstatin, and 1 μ g/ml aprotinin. When indicated, ionophores (10 μ M nigericin and 75 μ M monensin) were added. A 300- μ l aliquot of yeast lysate was incubated at 30 °C for 30 min in the presence of 1 mM HPTS. The appropriate volume of 8.5% phosphoric acid (0–7.9 μ l) or 1 M Tris solution (0–5.6 μ l) was added to adjust the pH to the desired values. All reactions were stopped on ice and centrifuged at 13,000 × *g* for 30 min at 4 °C to isolate the membranes. The membranes were again suspended in 500 μ l of reaction buffer A containing 20 mM *p*-xylylene-bispyridinium bromide (DPX) (Invitrogen, Molecular Probes). Fluorescence intensity (emission wavelength (λ_{em}) =

510 nm) was recorded at the excitation wavelength ($\lambda_{\text{ex}} = 300 - 500$ nm) by an FP-750 fluorometer (Jasco). The fluorescence of HPTS at $\lambda_{\text{ex}} = 417$ nm was applied to quantify the amount of HPTS trapped in MVB vesicles. For measurement of the pH in MVB vesicles, the fluorescence of HPTS at $\lambda_{\text{ex}} = 417$ and 463 nm was measured. For the standard curve, the fluorescence of HPTS was measured in pH calibration buffers containing DPX (50 mM MES, 50 mM HEPES, 75 mM KCl, 75 mM NaCl, 200 mM ammonium acetate, 10 mM NaN_3 , 10 mM 2-deoxy-D-glucose, 20 mM DPX, 10 μM nigericin, and 75 μM monensin at pH 5.5, 6.0, 6.5, 7.0, 7.5, 8.0, and 8.5).

OptiPrep Density Gradient Centrifugation—For the *in vitro* MVB assay, the mixtures obtained after incubation at 4 °C or 30 °C were centrifuged at $200,000 \times g$ for 1 h at 4 °C to isolate the membranes. The pellets were resuspended in 0.8% sorbitol-triethanolamine buffer (0.8% sorbitol, 10 mM triethanolamine, 1 mM EDTA- 2Na^+ , pH adjusted to 7.4 with acetic acid). The suspensions (150 μl) were supplemented with a solution (1050 μl) of 40% OptiPrep (Sigma), 0.8% sorbitol-triethanolamine buffer to a final concentration of 35% OptiPrep and then overlaid with 10 ml of 12–30% density gradient OptiPrep, 0.8% sorbitol-triethanolamine buffer. The samples were subjected to centrifugation at $100,000 \times g$ for 16 h at 4 °C, and 19 fractions of equal volume were collected from the top of each tube. The HPTS level in the fractions was measured with a fluorometer and analyzed by SDS-PAGE and immunoblotting.

Subcellular Fractionation—For determination of the amount of Vps27p bound to endosomal membranes, fractionation of proteins into membrane-associated pellet and soluble cytosolic fractions was performed as described for yeast lysate and membrane preparation. Yeast cells expressing Vps27p-TAP grown at 30 °C in YPAD medium were converted to spheroplasts by the addition of zymolyase. The resulting spheroplasts were suspended in reaction buffer A containing protease inhibitors, homogenized on ice by 10 passes through a 26 gauge needle with a 1-ml syringe, and then centrifuged twice at $400 \times g$ for 5 min at 4 °C. The resulting supernatant was used as the total fraction. The total fraction was further centrifuged at $13,000 \times g$ for 15 min at 4 °C to obtain the P13 pellet and S13 supernatant. The fractions were resolved by SDS-PAGE and analyzed by immunoblotting using anti-TAP and anti-Pep12p antibodies. Late endosome-localized t-SNARE (Pep12p) was examined as the endosomal membrane-associated control. To determine the pH dependence of the Snf7p-endosome interaction, a spheroplast of yeast cells expressing Snf7p-TAP was suspended in reaction buffer B containing protease inhibitors, homogenized on ice by 10 passes through a 26-gauge needle with a 1-ml syringe, and then centrifuged twice at $400 \times g$ for 5 min at 4 °C. An appropriate volume of 8.5% phosphoric acid (0–7.9 μl) or 1 M Tris solution (0–5.6 μl) together with ionophores (10 μM nigericin and 75 μM monensin) was then added to an equal volume of the resulting supernatants to adjust the pH to desired values. After incubation at 30 °C for 30 min, lysates were centrifuged at $13,000 \times g$ for 15 min at 4 °C for separation into the P13 pellet and S13 supernatant. The fractions were resolved by SDS-PAGE and analyzed by immunoblotting using anti-TAP antibody.

SDS-PAGE, Immunoblotting Analysis, and Antibodies—Protein samples were subjected to electrophoresis in 10 or 12.5% SDS-polyacrylamide gels. The separated proteins were transferred to a hydrophobic polyvinylidene fluoride filter (Millipore), which was incubated with 5% skim milk in PBST buffer (7.81 mM Na_2HPO_4 , 1.47 mM KH_2PO_4 , 137 mM NaCl, 2.68 mM KCl, and 0.1% Tween 20) and then exposed to primary antibodies. After multiple washes with PBST buffer, the membranes were incubated with horseradish peroxidase-conjugated secondary antibodies. Immunoreactive bands were visualized by the enhanced chemiluminescence method (GE Healthcare). Rabbit anti-TAP antibody was purchased from Open Biosystems. Mouse anti-Pep12p, Vph1p, and 3-phosphoglycerate kinase (Pgk1p) antibodies were purchased from Invitrogen, Molecular Probes. Goat anti-Pma1p antibody was purchased from Santa Cruz. Horseradish peroxidase-conjugated secondary antibodies against mouse and goat IgG were purchased from Jackson ImmunoResearch Laboratories or Vector Laboratories.

Fluorescence Microscopy—Yeast cells grown to log phase at 30 °C in APG medium were directly observed at room temperature in APG medium or pH calibration buffer under a fluorescence microscope (BX-51, Olympus) equipped with NIBA (for EGFP) or WIG (for FM4-64 and mCherry) filter sets. A UPlanApo 100 \times /NA 1.35 oil-immersion objective was used. Images were recorded using an ORCA-ER1394 digital camera (Hamamatsu Photonics) under the control of Aquacosmos software (Hamamatsu Photonics). For FM4-64 staining, yeast cells grown exponentially were harvested, suspended in fresh yeast extract/peptone/dextrose or APG medium ($\text{OD}_{600} = 10 - 20$), and incubated with FM4-64 dye (Invitrogen, Molecular Probes) at a final concentration of 4 μM . After incubation for 30 min, the cells were washed three times with yeast extract/peptone/dextrose or APG medium and then immediately observed by fluorescence microscopy (BX51, Olympus). All confocal images were acquired at room temperature with a laser scanning microscope (FV1000D, Olympus). Lysate from cells expressing Pep12p-mCherry incubated with HPTS was placed on a glass-bottom dish (Matsunami Glass) after the addition of 100 mM DPX. The sample was excited with an argon laser (488 nm) and a HeNe laser (543 nm), and the emission was collected at 500–530 nm for HPTS and at 580–680 nm for mCherry. Adobe Photoshop CS4 (Adobe) was used for data acquisition. For pH measurement, fluorescence was captured by a Fluoview FV1000D confocal laser scanning microscope (Olympus), as detailed below.

Measurement of Endosome Luminal and Cytoplasmic pH—To measure intracellular pH, images were obtained at room temperature using a Fluoview FV1000D confocal laser scanning microscope (Olympus) equipped with a UPlanSApo 100 \times /NA 1.40 oil immersion objective (Olympus). For measurement of endosome luminal pH, a late endosome-targeting ratiometric pH probe (Pep12p-EGFP-mCherry) was constructed by the fusion of two fluorescent proteins (EGFP-mCherry) to the C terminus of the late endosome-localized t-SNARE protein (Pep12p). Yeast cells expressing Pep12p-EGFP-mCherry were grown to log phase at 30 °C in APG (pH 5.5), medium and attached to a glass-bottom dish coated with concanavalin A.

Role of Nhx1p in MVB Formation

The samples were excited with an argon laser (488 nm) and a HeNe laser (543 nm), and the emissions were collected at 500–530 nm for EGFP and 580–680 nm for mCherry. For measurement of cytoplasmic pH, yeast cells expressing the cytoplasmic pH probe (pHluorin or pHluorin-Vps27p) were grown in APG medium to log phase at 30 °C and fixed on a glass-bottom dish coated with concanavalin A. The cells were sequentially excited with an LD laser (405 nm) and an argon laser (488 nm), and the emissions were collected at 500–600 nm. For the pH standard curve, the images were acquired in pH calibration buffers (50 mM MES, 50 mM HEPES, 75 mM KCl, 75 mM NaCl, 200 mM ammonium acetate, 10 mM Na₂CO₃, 10 mM 2-deoxy-D-glucose, 10 μ M nigericin, and 75 μ M monensin at pH 5.0, 5.5, 6.0, 6.5, and 7.0). All quantifications were performed on background-subtracted images of 50–100 cells using MetaMorph software (Molecular Devices).

RESULTS

Endosomal Na⁺/H⁺ Exchange Activity Is Required for Efficient Transport of Cps1p to the Vacuole Lumen—To investigate whether Nhx1p is required for the sorting of vacuolar proteins via the MVB pathway, the vacuolar delivery of carboxypeptidase S (Cps1p), a typical MVB cargo in yeast cells, was monitored (Fig. 1A). A precursor form of the yeast vacuolar enzyme Cps1p is synthesized as an integral membrane protein in the endoplasmic reticulum, transported directly from the Golgi complex to the endosomes, and sorted into the internal vesicles of the MVBs (36). Fusion of MVBs containing the precursor to the vacuole results in delivery of the precursor into the vacuole lumen, where the precursor is proteolytically cleaved and released from its transmembrane anchor to produce the soluble mature form of the enzyme (36). GFP-Cps1p, in which GFP is fused to the N terminus of the enzyme, was observed in the vacuole lumen in wild-type cells (Fig. 1A), indicating that GFP-Cps1p had been properly delivered. In *nhx1* Δ cells, although some of the GFP-Cps1p was present as diffuse fluorescence in the vacuolar lumen, most was mislocalized to a large punctate structure adjacent to the vacuole (Fig. 1A). These results suggest that Nhx1p is required for the efficient transport of Cps1p into the vacuole lumen. FM4-64, a fluorescent lipophilic dye that intercalates into the plasma membrane and is internalized into the vacuolar membrane by endocytosis, was localized in the limiting membrane of the vacuole in wild-type cells (Fig. 1A). In the class E *vps27* Δ mutant, FM4-64 is known to accumulate in an enlarged late endosome called a class E compartment (Fig. 1A; Ref. 37). In *nhx1* Δ cells, FM4-64 labeled one or two large punctate structures located adjacent to the vacuole, similar to the localization observed in *vps27* Δ cells (Fig. 1A). The signal of the mislocalized GFP-Cps1p colocalized with the FM4-64-labeled class E compartment, suggesting that deletion of *NHX1* causes impaired MVB formation.

Negatively charged residues are putatively involved in the ion-transport activity of Nhx1p (30). To confirm that Nhx1p activity is required for the correct delivery of GFP-Cps1p into the vacuole lumen, the intracellular localization of GFP-Cps1p was analyzed in *nhx1* Δ cells transformed with plasmids carrying either wild-type *NHX1* or mutant Nhx1p (Nhx1p-E225Q/D230N), in which two negatively charged residues, Glu-225 and

Asp-230, were replaced by Gln and Asn. Although the growth of yeast cells expressing wild-type Nhx1p is resistant to hygromycin, the expression of mutant Nhx1p induced hygromycin sensitivity (supplemental Fig. S1), confirming that mutant Nhx1p has lost ion-transport activity. In *nhx1* Δ cells, expression of wild-type Nhx1p restored localization of GFP-Cps1p to the vacuole lumen, whereas expression of mutant Nhx1p did not affect the abnormal accumulation of GFP-Cps1p (Fig. 1B). These observations support the notion that the ion-transport activity of Nhx1p is required for proper delivery of Cps1p into the vacuole lumen via the MVB pathway.

Establishment of an in Vitro Biochemical Assay System for MVB Formation—In previous MVB studies, internal vesicles in the endosomes have been observed by electron microscopy (EM) (15, 38). However, quantification of MVB formation by EM analysis is limited. Because *nhx1* Δ cells show a weaker phenotype than *vps27* Δ or *snf7* Δ cells (Fig. 1A), a more sensitive quantitative assay for MVB formation was needed. To assess the contribution of Nhx1p to MVB formation, a cell-free biochemical assay system was developed. MVB vesicles form by inward budding of the endosomal membrane into the lumen of the endosome. Assuming that soluble cytoplasmic materials trapped in the MVBs become inaccessible from the cytoplasm, yeast cell lysate containing endocytic vesicles was prepared (as described under “Experimental Procedures”). The lysates were then incubated with the water-soluble and membrane-impermeable fluorescence dye HPTS in buffer containing ATP-regenerating solution at 30 °C (Fig. 2A). The reaction was stopped by placing the samples on ice, and the membrane vesicles were isolated by centrifugation and resuspended. To quench the residual fluorescence of HPTS outside the MVBs, membrane-impermeable DPX was added to the buffer (Fig. 2A). Thus, the fluorescence of the entrapped HPTS could be measured by fluorescence microscopy. In control lysates, HPTS-derived fluorescent signals were observed as a few punctate structures after incubation for 3 min at 30 °C (Fig. 2C). The fluorescence intensity of the HPTS signal increased after a longer incubation period of 30 min (Fig. 2C). When lysates prepared from yeast cells expressing Pep12p-mCherry (Fig. 2B) as a marker of late endosomes were used, most of the HPTS signal colocalized with the late endosome marker (Fig. 2C). HPTS fluorescence measured at 510 nm is pH-dependent when excited at 463 nm but pH-independent when excited at 417 nm (Fig. 2D). Thus, the fluorescence of HPTS at $\lambda_{\text{ex}} = 417$ nm was applied to quantify HPTS entrapped in MVB vesicles (Fig. 2E). After incubation for 30 min at 30 °C, the HPTS signal was approximately 5 times higher than at 4 °C, and DPX-protected HPTS signals disappeared in the presence of detergent (Fig. 2E). Freeze-thawing did not increase the HPTS signal after incubation at 30 °C (Fig. 2E). These observations strongly suggest that the HPTS was sequestered into membrane vesicles.

To further characterize dye uptake, yeast lysates incubated with HPTS were fractionated by OptiPrep density gradient centrifugation (Fig. 3, A and B). Most of the HPTS-derived fluorescence signals after incubation at 4 °C were detected in the bottom fractions (fractions 17–19). However, after incubation at

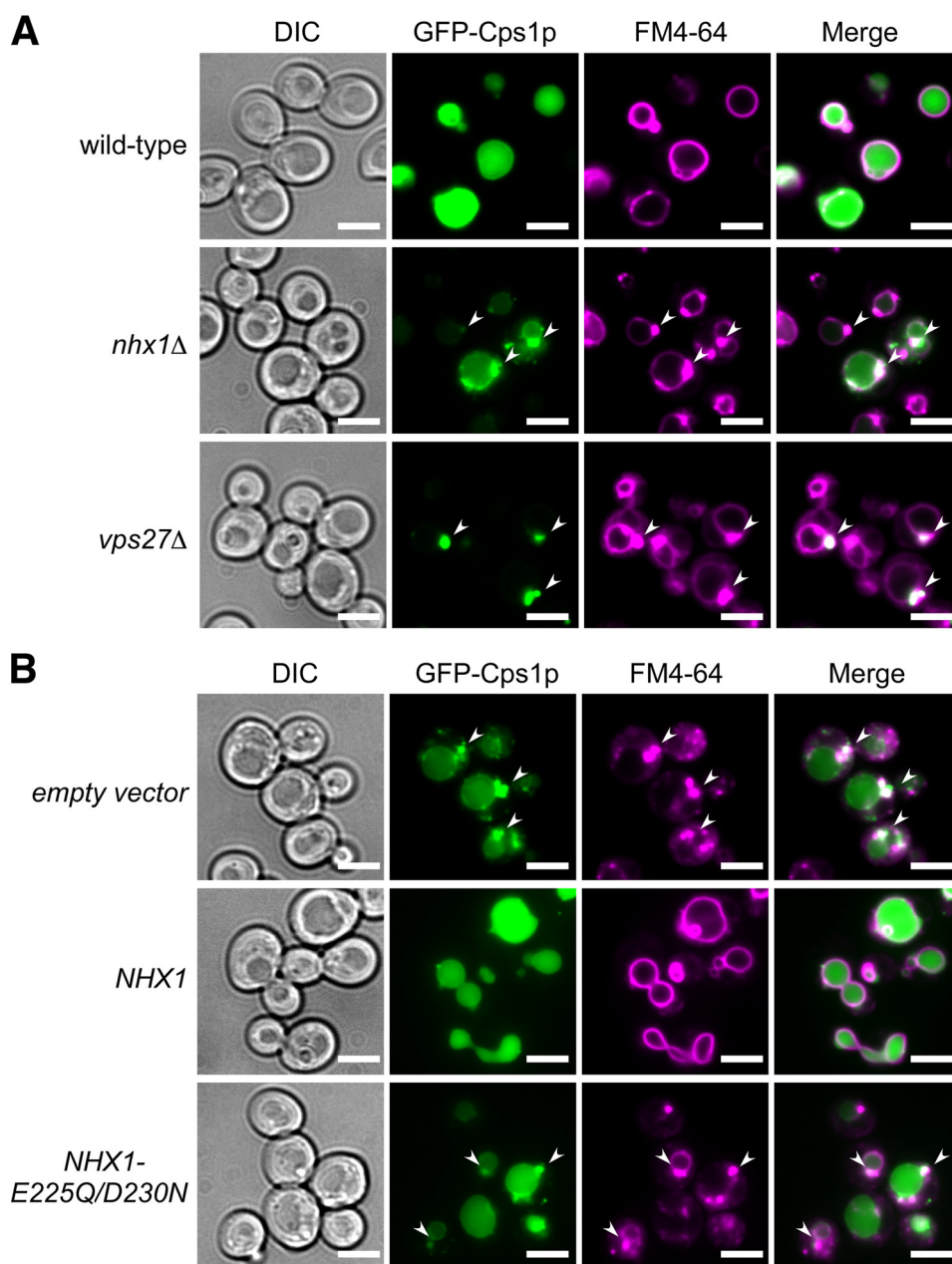


FIGURE 1. Nhx1p is required for GFP-Cps1p transport into the vacuolar lumen via the MVB pathway. A, intracellular localization of GFP-Cps1p and FM4-64 is shown. Wild-type (BY4742), *nhx1Δ* (MKY0804), and *vps27Δ* (MKY0806) yeast strains transformed with pRS316GAP1p-GFP-CP51 were grown to logarithmic phase in APG medium adjusted to pH 5.5 and stained with FM4-64 dye. The intracellular localization of GFP-Cps1p (green) and FM4-64 (magenta) was observed under a fluorescence microscope. Arrows indicate class E compartments. Scale bars, 5 μ m. B, shown is the effect of Nhx1p activity on GFP-Cps1p transport into the vacuolar lumen. Yeast strain *nhx1Δ* cells (MKY0614) expressing GFP-Cps1p were transformed with pRS314 (empty vector), pRS314-NHX1-FLAG (*NHX1*), or pRS314-NHX1-E225Q/D230N-FLAG (*NHX1-E225Q/D230N*). The cells were grown to logarithmic phase in APG medium (pH 5.5) and stained with FM4-64 dye. The intracellular localization of GFP-Cps1p (green) and FM4-64 (magenta) was observed under a fluorescence microscope. Arrows indicate class E compartments. Scale bars, 5 μ m.

30 °C, fluorescence was observed in the top fractions (fractions 1–4) as well as the bottom fractions (Fig. 3A). Immunoblotting experiments using antibodies against several organelle-specific markers indicated that the top fractions contained the organelle membranes of the late endosomes (Pep12p) and vacuoles (Vph1p) but not the plasma membranes (Pma1p) or cytosol (3-phosphoglycerate kinase) (Fig. 3B). In addition, in *in vitro* assay, the endosome-enriched membrane fraction (P13 membranes) showed significant HPTS uptake (Fig. 3C). These results indicate that the increasing HPTS signals during incu-

bation correspond to the uptake of dye into the late endosomes. A major characteristic of endosomes is the acidic pH of their lumen. However, the pH of the internal vesicles is not known. The ratio of HPTS fluorescence ($\lambda_{em} = 510$ nm) at $\lambda_{ex} = 417$ and 463 nm can be fit to the sigmoid curve between pH 5.5 and 8.5.⁴ From this calibration curve, the pH surrounding HPTS entrapped in late endosomes during the MVB formation assay

⁴ K. Mitsui, Y. Koshimura, Y. Yoshikawa, M. Matsushita, and H. Kanazawa, unpublished data.

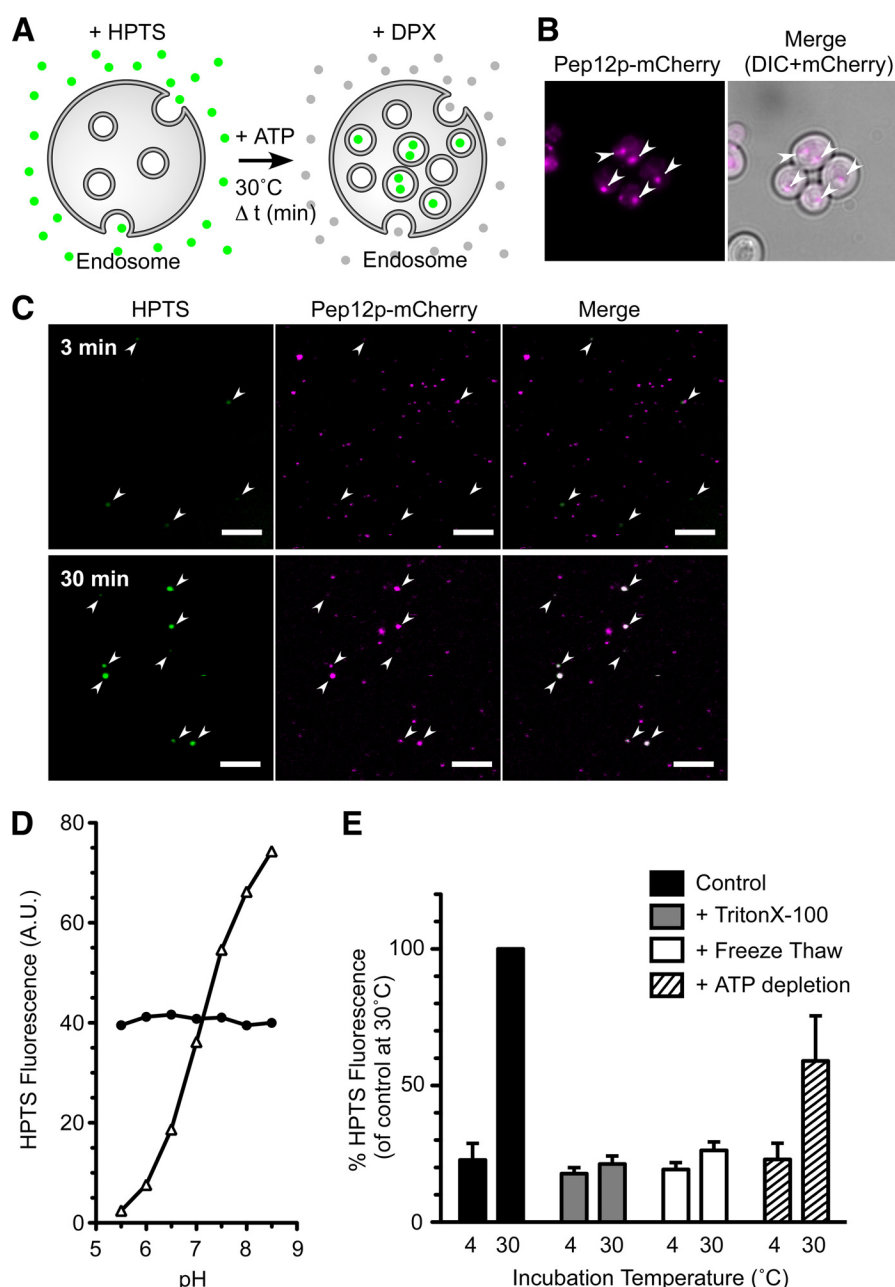


FIGURE 2. Temperature- and ATP-dependent HPTS uptake into membrane vesicles. *A*, shown is a schematic representation of the cell-free assay for MVB formation. Yeast lysates were incubated with HPTS (green circles) at 30 °C in the presence of ATP. After incubation, HPTS taken up into the endosomes was protected from DPX, whereas HPTS that remained outside the endosomes was quenched by DPX (gray circles). *B*, shown is intracellular localization of Pep12p-mCherry. Wild-type cells (BY4742) transformed with pRS316GAP1p-PEP12-mCherry were grown to logarithmic phase in APG medium (pH 5.5) at 30 °C and observed with a fluorescence microscope. Arrows indicate the location of signals for Pep12-mCherry. Scale bars, 5 μ m. *C*, yeast cells (BY4742) expressing Pep12p-mCherry were grown to early logarithmic phase in APG medium (pH 5.5) at 30 °C, converted to spheroplasts, and disrupted as described under "Experimental Procedures." The resulting lysates were incubated with 1 mM HPTS at 30 °C for the indicated time. After treatment with DPX, the lysates were immediately observed under a laser confocal microscope. Arrows indicate the positions of HPTS signals. Scale bars, 5 μ m. *D*, shown is pH dependence of HPTS fluorescence. Fluorescence intensity of HPTS was measured with excitation at 417 nm (closed circle) and 463 nm (open triangle) in a 150 mM NaCl solution adjusted to pH 5.5, 6.0, 6.5, 7.0, 7.5, 8.0, or 8.5 with 20 mM MES (pH 5.5–6.5) and HEPES (pH 7.0–8.5). A.U., absorbance units. *E*, shown is characterization of HPTS uptake into late endosomes. Lysate prepared from wild-type cells (BY4742) was incubated with 1 mM HPTS dye for 30 min at 4 °C or 30 °C in the presence of an ATP-regenerating solution (black bars, control) or without ATP (hatched bars, + ATP depletion). The amount of HPTS trapped in late endosomes was quantified by a fluorometer after the addition of DPX. Lysates with detergent (gray bars, + Triton X-100) or freeze-thawed (white bars, + Freeze Thaw) were used in this assay. Data express the HPTS level relative to control at 30 °C and represent the means \pm S.D. of at least three independent experiments.

was calculated to be 6.99 ± 0.06 , similar to that of the reaction buffer (pH 7.2). This result suggests that the pH of MVB vesicles is maintained at cytoplasmic pH *in vivo*. This result supports that HPTS was not incorporated into the endosomal lumen and that HPTS was most likely present in the internal vesicles of the MVBs.

Vps4p has ATPase activity and is directly involved in MVB formation (14). When ATP in the reaction buffer was completely hydrolyzed by apyrase, the efficiency of HPTS uptake was reduced by $\sim 40\%$ (Fig. 2*E*). Together, these results indicate that HPTS uptake is temperature- and ATP-dependent, which is consistent with MVB formation.

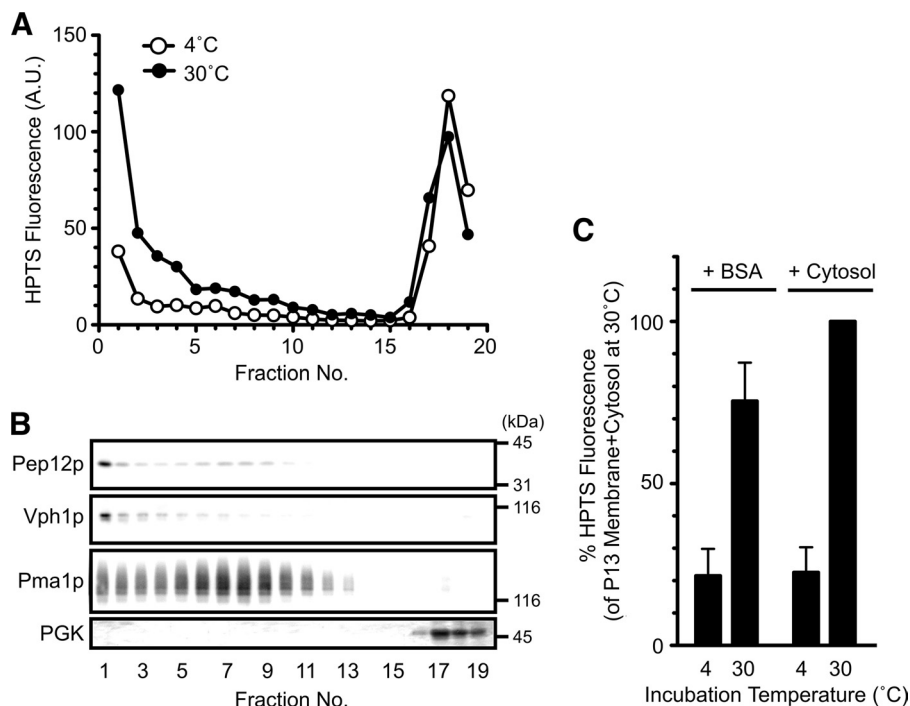


FIGURE 3. HPTS is incorporated into endosomal membranes during incubation. *A* and *B*, wild-type cells (BY4742) were grown to logarithmic phase in YPAD medium at 30 °C, converted to spheroplasts, and disrupted as described under "Experimental Procedures." The resulting lysate was subjected to 12–30% OptiPrep density gradient centrifugation after incubation with HPTS at 4 or 30 °C for 30 min in the presence of ATP-regenerating solution. Next, 19 fractions of equal volume were collected from the top of the tube. The HPTS level in each fraction was quantified with a fluorometer (*A*) and analyzed by SDS-PAGE and immunoblotting using anti-Pep12p (late endosome), anti-Vph1p (vacuole), anti-Pma1p (plasma membrane), and anti-3-phosphoglycerate kinase (cytoplasm) antibodies (*B*). A.U., absorbance units. *C*, wild-type cells (BY4742) were grown to early logarithmic phase in YPAD medium, converted to spheroplasts, and disrupted. The resulting lysate was further centrifuged at $13,000 \times g$ for 15 min to obtain endosome-enriched membranes (P13 membranes). The P13 membranes were incubated with BSA or a cytosolic fraction in the presence of the ATP-regenerating solution at 4 or 30 °C for 30 min. HPTS uptake was quantified with a fluorometer. Data express the HPTS level relative to that of the P13 membrane + cytosol at 30 °C and represent the means \pm S.D. of at least three independent experiments.

Loss of the Endosomal Na^+/H^+ Exchanger Impairs MVB Formation—To confirm that the *in vitro* assay system established here reflects MVB formation *in vivo*, the effect of depletion of Vps27p and Snf7p was assessed (Fig. 4). The *vps27Δ* and *snf7Δ* cells are defective in internal vesicle budding *in vivo* (3, 8). In these cells uptake of HPTS increased in a time-dependent manner and reached a plateau at 30 min (Fig. 4A). Lysates from *vps27Δ* and *snf7Δ* cells exhibited a decrease in HPTS uptake after incubation for 30 min (Fig. 4B). Furthermore, when wild-type cytosol (including cytosolic ESCRT proteins) was added to the P13 membranes, HPTS uptake was significantly increased (Fig. 3C). These results suggest that *in vitro* MVB formation is inhibited upon loss of ESCRT proteins (Vps27p or Snf7p) and support the notion that the HPTS uptake in this assay depends on the formation of MVB vesicles in endosomes. MVB formation was also measured in *nhx1Δ* cells (Fig. 4). HPTS uptake in *nhx1Δ* cells was reduced by ~30% compared with wild-type cells (Fig. 4, A and B). These results strongly suggest that Nhx1p is required for the efficient formation of MVB vesicles.

Loss of Nhx1p Activity Affects the Endosomal Localization of ESCRT Proteins—Because MVB formation requires the ordered recruitment of ESCRT-0, -I, -II, and -III complexes to the endosome (3), the role of Nhx1p in the recruitment of ESCRTs to the endosomal membranes was analyzed (Fig. 5). When ESCRT-0/GFP-Vps27p was overexpressed under the control of the *GAP1* promoter, no difference in intracellular localization was observed between wild-type and *nhx1Δ* cells.⁴

Next, GFP-Vps27p was expressed under the control of its own promoter in a low-copy plasmid. In wild-type cells, GFP-Vps27p localized to smaller and more punctate structures (Fig. 5A) than when it was overexpressed. GFP-Vps27p partially colocalized with Nhx1p-mCherry at the punctate structures, which presumably correspond to endosomes (supplemental Fig. S3A). In *nhx1Δ* cells, GFP-Vps27p displayed increased cytoplasmic distribution, although GFP-Vps27p localization at one or two large punctate structures (class E compartments) was also observed (Fig. 5A). Vps27p bound to endosomal membranes was quantified in lysates prepared from wild-type and *nhx1Δ* cells containing chromosomally TAP-tagged Vps27p by immunoblot analysis using anti-TAP antibody (Fig. 5, B and C). The lysates were separated by centrifugation into the P13 fraction, which contained membranes of vacuoles and endosomes, and the S13 fraction, which contained soluble proteins and other organelle membranes (as described under "Experimental Procedures"). In wild-type cells, most Vps27p was detected in the P13 fraction (Fig. 5B). Lysate from *nhx1Δ* cells exhibited a significant shift in Vps27p distribution to the S13 fraction (Fig. 5B). The amount of Vps27p in the P13 fraction decreased from 80% in wild-type cells to 55% in *nhx1Δ* cells (Fig. 5C). This suggests that Nhx1p is involved in the recruitment of Vps27p to the endosomal membrane.

Next, the intracellular localization of ESCRT-III/Snf7p-GFP, which is recruited to the membrane by ESCRT-0/Vps27p, was assessed. As expected, the intracellular localization of Snf7p-

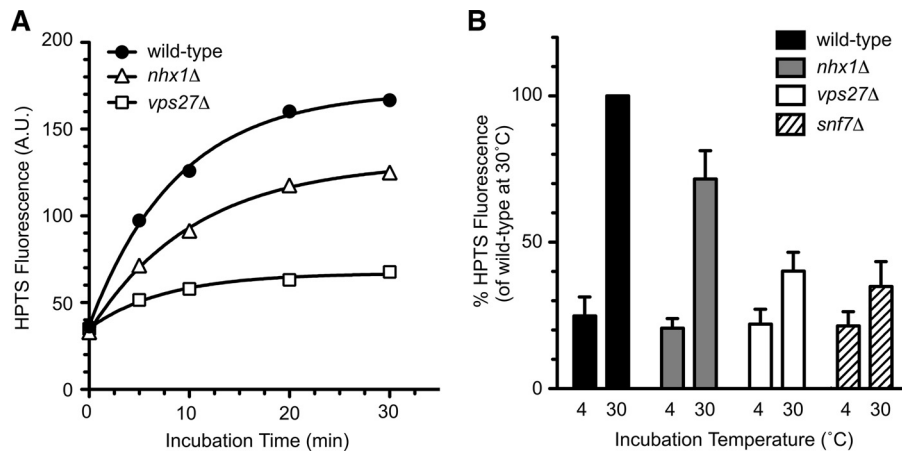


FIGURE 4. Nhx1p mediates the formation of MVB vesicles in endosomes. Wild-type (BY4742), *nhx1Δ* (MKY0804), *vps27Δ* (MKY0806), and *snf7Δ* (MKY1001) cells were grown to early logarithmic phase in YPAD medium at 30 °C, converted to spheroplasts, and disrupted as described under "Experimental Procedures." The resulting lysates were incubated with 1 mM HPTS in the presence of ATP-regenerating solution. **A**, after incubation at 30 °C for the indicated time periods, HPTS levels were quantified with a fluorometer. **B**, HPTS levels from lysates of wild-type (black bars), *nhx1Δ* (gray bars), *vps27Δ* (white bars), and *snf7Δ* (hatched bars) cells were quantified after incubation for 30 min at 4 °C or 30 °C. Data express the HPTS level relative to wild-type cells at 30 °C and represent the means \pm S.D. of at least four independent experiments.

GFP was significantly affected by disruption of the *NHX1* gene (Fig. 5D). Although Snf7p-GFP was distributed in punctate structures near the vacuole and vacuolar membrane in wild-type cells, in *nhx1Δ* cells it was localized to large punctate structures (class E compartments) as in *vps27Δ* cells (Fig. 5D). Importantly, cell surface localization of Snf7p-GFP was clearly observed in *nhx1Δ* and *vps27Δ* cells but not in wild-type cells (Fig. 5D). Although the physiological significance of Snf7p localization to the cell surface is not clear, this observation indicates that the loss of Nhx1p resulted in defective recruitment of Snf7p to the endosomal membrane. In addition, correct localization of Snf7p-GFP was dependent on the ion-transporting activity of Nhx1p (Fig. 5E). When colocalization of Nhx1p with ESCRT proteins was analyzed, Nhx1p was partially colocalized with Vps27p in the endosomal membrane but not with Snf7p (supplemental Fig. S3, A and B). These observations suggest that Nhx1p activity regulates Vps27p function at the endosomal membrane.

Recruitment of Vps27p to the Endosomal Membranes Is Controlled by pH—To assess the pH dependence of MVB formation on the endosomal localization of ESCRT complexes, Vps27p (ESCRT-0), Vps23p (ESCRT-I), Vps36p (ESCRT-II), and Snf7p (ESCRT-III) were chosen as representative components of each known ESCRT complex. Yeast cells expressing each ESCRT protein tagged with EGFP under the control of the *GAP1* promoter were suspended in ionophore buffer with a pH range from 5.5 to 7.5 (as described under "Experimental Procedures"). Localization was observed immediately to examine the direct effect of pH on the interaction between ESCRTs and endosomal membranes. GFP-Vps27p exhibited obvious pH-dependent endosomal localization. In yeast cells grown in normal medium (APG medium with a pH of 5.5), GFP-Vps27p localized to the large punctate structure (Fig. 6A), similar to the Pep12p-positive compartment seen in Fig. 2B. After suspension in ionophore buffer at pH 5.5, GFP-Vps27p was strongly targeted to the endosomal membranes (Fig. 6B). When the pH was progressively increased, the amount of membrane-bound GFP-Vps27p diminished, and diffused GFP-Vps27p appeared in the

cytoplasm (Fig. 6B). Vps27p binds directly to endosomal lipid phosphatidylinositol 3-phosphate (PI(3)P) through its FYVE domain (a zinc finger domain highly conserved in Fab1p, YOTB, Vac1p, and EEA1 proteins (10)). In agreement with this, the interaction of the FYVE domain in the mammalian EEA1 protein with a PI(3)P lipid is pH-dependent (39). In wild-type cells, GFP-Vps27p-H190A/H191A, in which the His-190 and His-191 residues in the FYVE domain were replaced by Ala residues (39, 40), was distributed in the cytoplasm at all pH levels (Fig. 6, C and D), indicating that the interaction of Vps27p with PI(3)P in the endosomal membrane via its FYVE domain is pH-dependent. In contrast, the endosomal localization of other ESCRT proteins (Vps23p, Vps36p, and Snf7p) was not affected by pH (supplemental Fig. S2). When yeast cells expressing Snf7p-TAP were exposed to the ionophore buffers, Snf7p-TAP levels bound to endosomal membranes did not change without incubation (supplemental Fig. S3C; wild type, 0 min), in agreement with microscopic observations (supplemental Fig. S2C). However, after longer exposure, endosomal localization of Snf7p-TAP changed in a pH-dependent manner similar to Vps27p (supplemental Fig. S3C, wild type, 30 min). No pH dependence of membrane-associated Snf7p was observed in *vps27Δ* cells (supplemental Fig. S3C, *vps27Δ*, 30 min). These results indicate that pH-dependent recruitment of Vps27p to endosomes affects the endosomal targeting of downstream ESCRT proteins, such as Snf7p.

In Vitro MVB Formation Is pH-dependent—To confirm whether the change in ESCRT recruitment to the endosomal membrane affected by pH causes defective formation of MVB vesicles in the endosome, the pH dependence of *in vitro* MVB formation was assessed (Fig. 7). HPTS uptake was quantified for endosomes in which the outside pH was clamped at a desired level. HPTS uptake gradually decreased as the pH increased (Fig. 7A). These results indicated that efficient MVB formation was maintained at an acidic pH but was inhibited at neutral pH and are consistent with the pH dependence of the Vps27p-endosome interaction (Fig. 6). However, the possibility existed that the pH gradient between the outside and the inside endo-

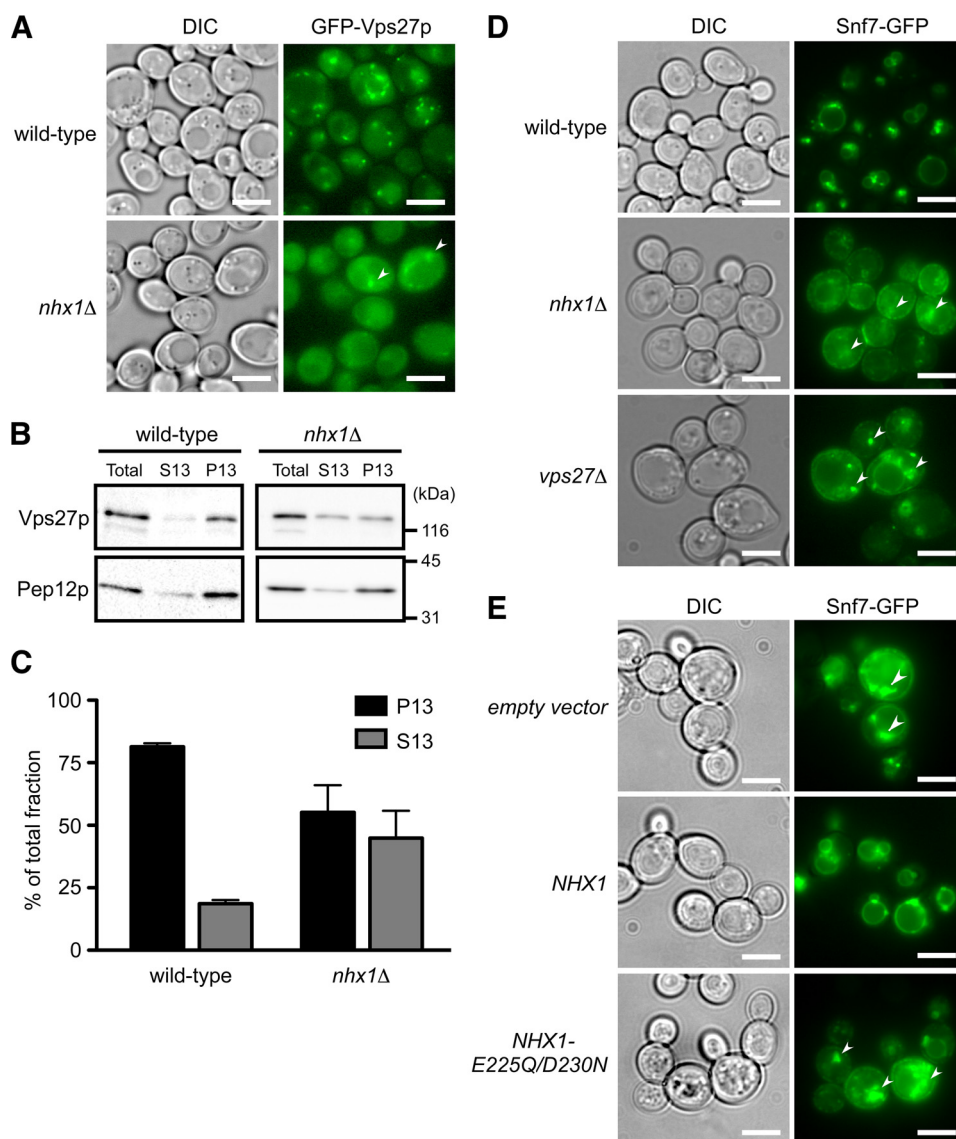


FIGURE 5. Nhx1p activity is required for the endosomal recruitment of ESCRT proteins. *A*, intracellular localization of GFP-Vps27p in wild-type and *nhx1*Δ cells is shown. Wild-type (BY4742) or *nhx1*Δ (MKY0804) cells expressing GFP-Vps27p (pRS316-GFP-VPS27) with its own promoter and a low-copy plasmid were grown to logarithmic phase in APG medium (pH 5.5) at 30 °C and then observed with a fluorescence microscope. Arrows indicate class E compartments. Scale bars, 5 μm. *B*, subcellular fractionation and immunoblotting analysis of wild-type (VPS27-TAP) or *nhx1*Δ (YYY01) cells expressing Vps27p-TAP is shown. Lysate (total) was separated into a membrane-associated pellet (P13) and soluble cytosolic (S13) fraction. Each fraction was resolved by SDS-PAGE and analyzed by immunoblotting using anti-TAP and anti-Pep12p antibodies. Pep12p was used as the endosomal membrane-associated control. *C*, the intensity of the immunoreactive bands was quantified using Image J software, and the amounts of Vps27p-TAP in the P13 (black bars) and S13 (gray bars) fractions are shown as the relative intensity (%) compared with Vps27p-TAP in the total fraction. Data shown are the average of three independent experiments ± S.D. *D*, shown is intracellular localization of the ESCRT-III protein Snf7p-GFP. Wild-type (BY4742), *nhx1*Δ (MKY0804), and *vps27*Δ (MKY0806) cells transformed with pRS316-SNF7-GFP were grown to the logarithmic phase in APG medium (pH 5.5) and observed with a fluorescence microscope. Arrows indicate the class E compartments. Scale bars, 5 μm. *E*, contribution of Nhx1p activity to Snf7-GFP localization is shown. *nhx1*Δ (MKY0614) cells expressing Snf7p-GFP were transformed with pRS314 (empty vector), pRS314-NHX1-FLAG (*NHX1*), or pRS314-NHX1-E225Q/D230N-FLAG (*NHX1-E225Q/D230N*). The cells were grown to logarithmic phase in APG medium (pH 5.5) and observed with a fluorescence microscope. Arrows indicate the class E compartments. Scale bars, 5 μm.

some was required for MVB formation. Therefore, the assay was repeated in the presence of two proton ionophores, nigericin and monensin, in order to dissipate the pH gradient across the endosomal membranes. The result was the same (Fig. 7*B*), indicating that a transmembrane pH gradient is not required. These observations imply that the *in vitro* formation of MVB vesicles depends on the outside pH of endosomes but not on the inside pH.

The Cytoplasmic Surface of the Endosome Is Acidified Compared with the Overall Cytoplasmic Space—GFP-Vps27p was not preferentially targeted to the endosomal membranes when

the pH of the buffer was 7.0, similar to the cytoplasmic pH of yeast cells (Fig. 6*B*). Therefore, the pH was measured in the bulk cytoplasm and at the cytoplasmic surface of the endosome where Vps27p is localized (Fig. 8). Free pHluorin or pHluorin-fused Vps27p (pHluorin-Vps27p) was overexpressed in yeast cells, as low level expression of the probe did not produce sufficient fluorescence for ratio imaging analysis. In wild-type cells, free pHluorin or pHluorin-Vps27p was correctly localized in the cytoplasm or the late endosome, respectively (Fig. 8, *A* and *B*). Based on ratio imaging analysis of fluorescence at $\lambda_{\text{ex}} = 405$ nm and $\lambda_{\text{em}} = 488$ nm, the pH at the Vps27p-bound cyto-

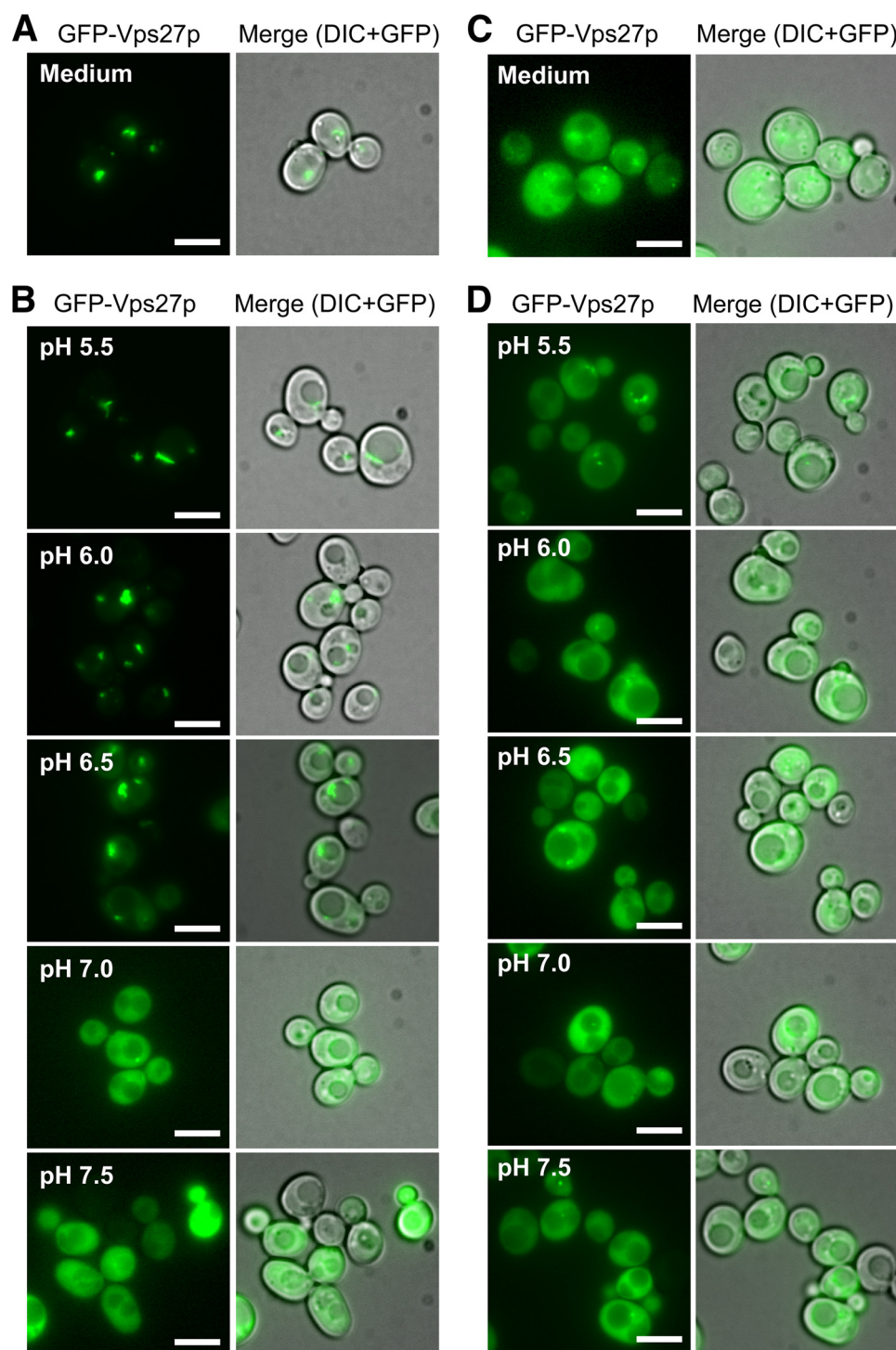


FIGURE 6. Interaction of GFP-Vps27p with the endosomal membrane depends on intracellular pH. A, intracellular localization of GFP-Vps27p in growing cells is shown. Yeast cells (BY4742) transformed with pRS316GAP1p-GFP-VPS27 were grown to logarithmic phase in APG medium (pH 5.5) at 30 °C and observed with a fluorescence microscope. Scale bars, 5 μ m. B, pH dependence of GFP-Vps27 localization is shown. Yeast cells (BY4742) expressing GFP-Vps27p were collected by centrifugation and resuspended in ionophore buffers adjusted to the indicated pH. Distribution of GFP-Vps27p was immediately observed under a fluorescence microscope. Scale bars, 5 μ m. C, intracellular localization of mutant GFP-Vps27p-H190A/H191A in growing cells. Yeast cells (BY4742) transformed with pRS316GAP1p-GFP-VPS27-H190A/H191A were grown to logarithmic phase in APG medium (pH 5.5) at 30 °C and observed with a fluorescence microscope. Scale bars, 5 μ m. D, shown is pH dependence of mutant GFP-Vps27-H190A/H191A localization. Yeast cells (BY4742) expressing GFP-Vps27p-H190A/H191A were collected by centrifugation and resuspended in ionophore buffer adjusted to the indicated pH. Distribution of the mutant GFP-Vps27p was immediately observed under a fluorescence microscope. Scale bars, 5 μ m.

plasmic surface was significantly more acidic (6.73 ± 0.08) than the pH of the bulk cytoplasm (7.02 ± 0.11) in cells expressing free pHluorin (Fig. 8D). Mutant pHluorin-Vps27p-H190A/H191A, which did not bind to the endosomal membrane,

showed the same diffused cytoplasmic distribution⁴ as the mutant GFP-Vps27p (Fig. 6C). When mutant Vps27p was used as a pH probe, the pH of the cytoplasm was 6.96 ± 0.14 (Fig. 8D). These results indicate that the cytoplasmic surface pH of

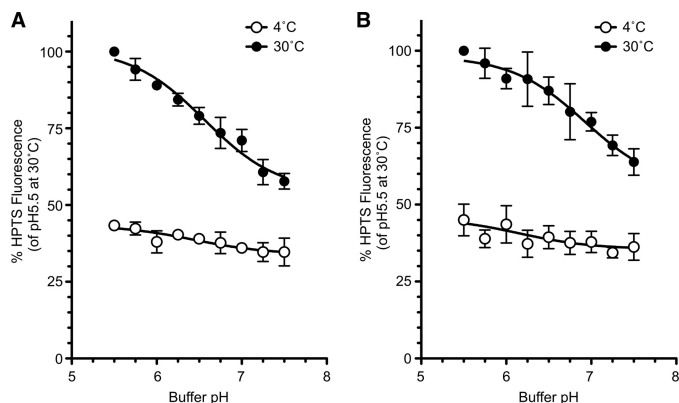


FIGURE 7. *In vitro* MVB formation is pH-dependent. A and B, yeast cells (BY4742) were grown to early logarithmic phase in YPAD medium, converted to spheroplasts, and disrupted as described under "Experimental Procedures." The resulting lysate was incubated with 1 mM HPTS for 30 min at 4 °C (open circles) or 30 °C (closed circles) at the indicated pH, and trapped HPTS levels were quantified. The assays were performed in the absence of ionophores (A) or in the presence of ionophores (B). Data are expressed as the HPTS levels relative to pH 5.5 at 30 °C and represent the means \pm S.D. of at least three independent experiments.

the endosome is more acidic than the overall cytoplasmic pH and suggest that acidification of the endosomal surface permits Vps27p to interact with the endosomal membrane.

The contribution of Nhx1p activity to the cytoplasmic surface pH of endosomes was then analyzed (Fig. 8). Because a small amount of Vps27p still localized in the class E-like endosomes in *nhx1Δ* cells (Fig. 5, A–C), pHluorin-Vps27p was used to measure the endosomal surface pH. In *nhx1Δ* cells, overexpressed pHluorin-Vps27p was observed in late endosomes (Fig. 8B). The pH of endosomal surface tended to increase upon the loss of Nhx1p (Fig. 8D). However, no significant difference between wild-type and *nhx1Δ* cells was observed in the overall cytoplasmic pH (Fig. 8D). These results could indicate that if a difference in pH between these strains does exist, it is not large enough to detect by the present approach. This will be further addressed under "Discussion."

Role of Luminal pH Regulation by Nhx1p in MVB Formation—Previous studies have suggested that the luminal pH of organelles is involved in vesicle formation and membrane fusion and affects membrane trafficking (41–44). For example, acidification of the endosomal lumen has been reported to regulate the recruitment of Arf1 or Arf6-GEF (ARNO), known to control the formation and budding of transport vesicles, to the cytoplasmic surface of endosomes (42–44). Therefore, the role of luminal pH regulation by Nhx1p in MVB formation was examined. Because a technique for measurement of the endosome luminal pH was not available in yeast cells, Pep12-EGFP-mCherry was constructed as a ratiometric pH probe targeted to the lumen of late endosomes (shown schematically in Fig. 9A). This chimeric protein, consisting of the endosomal t-SNARE protein (Pep12p) and tandem fluorescent proteins (EGFP and mCherry), localized to the late endosomes in wild-type cells, as expected (Fig. 9B). In *nhx1Δ* cells, Pep12p-EGFP-mCherry localized to larger punctate structures, possibly class E compartments (Fig. 9B). When yeast cells were suspended in pH calibration buffer containing ionophores, the ratio of the fluorescence intensity of EGFP (pH-dependent) to that of mCherry (pH-independent) increased linearly from pH 5.0 to 7.0

(Fig. 9C). Although wild-type cells showed a luminal pH of 6.36 ± 0.08 , *nhx1Δ* cells showed a reduction in luminal pH to 6.08 ± 0.09 (Fig. 9D). These results indicate that Nhx1p contributes to the regulation of endosome luminal pH by means of proton leakage from the endosome, as do organellar NHEs in mammalian cells (24, 25). Lowering the pH of the endosome lumen would not account for the impaired MVB formation in *nhx1Δ* cells because MVB formation observed *in vitro* was enhanced by acidic pH, as shown in Fig. 7B.

DISCUSSION

Previous genetic and morphological studies of yeast mutant cells revealed that Nhx1p is a class E protein (2, 3, 30); however, the functional role of Nhx1p in MVB formation has not been reported because no direct assay system for MVB formation was available. Here, we established an *in vitro* biochemical assay that monitors the formation of internal vesicles in the MVB of yeast cells (Figs. 2–4). This assay provided the first direct demonstration that Nhx1p contributes to MVB formation (Fig. 4). This assay system also enabled us to assess the contribution of a putative regulatory factor in MVB formation. Loss of Nhx1p decreased MVB formation by $\sim 30\%$, indicating that Nhx1p activity is important, but not essential, for MVB formation (Fig. 4). This is consistent with the fact that in *nhx1Δ* cells, a small population of Cps1p is correctly delivered to the lumen of the vacuole (Fig. 1A) and that Vps27p remained bound to the membrane (Fig. 5, A–C).

In this study we showed that Nhx1p activity directly regulates the recruitment of ESCRTs such as Vps27p and Snf7p to the endosomal membrane (Fig. 5). These findings suggest that the reduced recruitment of ESCRTs in *nhx1Δ* cells is the cause of impaired MVB formation. Organellar-type NHEs, including Nhx1p, are likely to mediate electroneutral exchange of sodium (or potassium) ion for protons (25, 45). Therefore, the loss of Nhx1p activity resulted in a shift in intracellular sodium, potassium, and proton concentrations. However, Nhx1p activity does not noticeably change endosomal or cytosolic Na^+ and K^+ concentrations, because of the much higher concentration of Na^+ or K^+ than H^+ in cells (46, 47). Thus, we considered the potential importance of pH in MVB formation. We found that the interaction between ESCRT-0/Vps27p and the endosomal membrane was enhanced by the acidic environment of the cytoplasmic surface of the endosome (Figs. 6 and 8) and that MVB formation was dependent on the pH outside of the endosome (Fig. 7). The most significant change in GFP-Vps27p distribution between the endosomal membrane and the cytoplasm occurred at a physiological pH range of 6.0–7.0 (Fig. 6B). This result is consistent with the pH dependence of *in vitro* formation of MVB (Fig. 7), suggesting the physiological relevance of pH sensing by the Vps27p-FYVE domain in MVB formation. Based on these results, we propose a possible pH-based model for the role of Nhx1p in MVB formation. First, Nhx1p alkalizes the endosomal lumen by proton efflux from the lumen and concomitantly acidifies the endosomal surface. This local acidification may then serve as a trigger for proper Vps27p recruitment to the endosomal membrane.

We were not able to detect an obvious contribution of Nhx1p to acidification at the endosomal surface (Fig. 8D). At first this

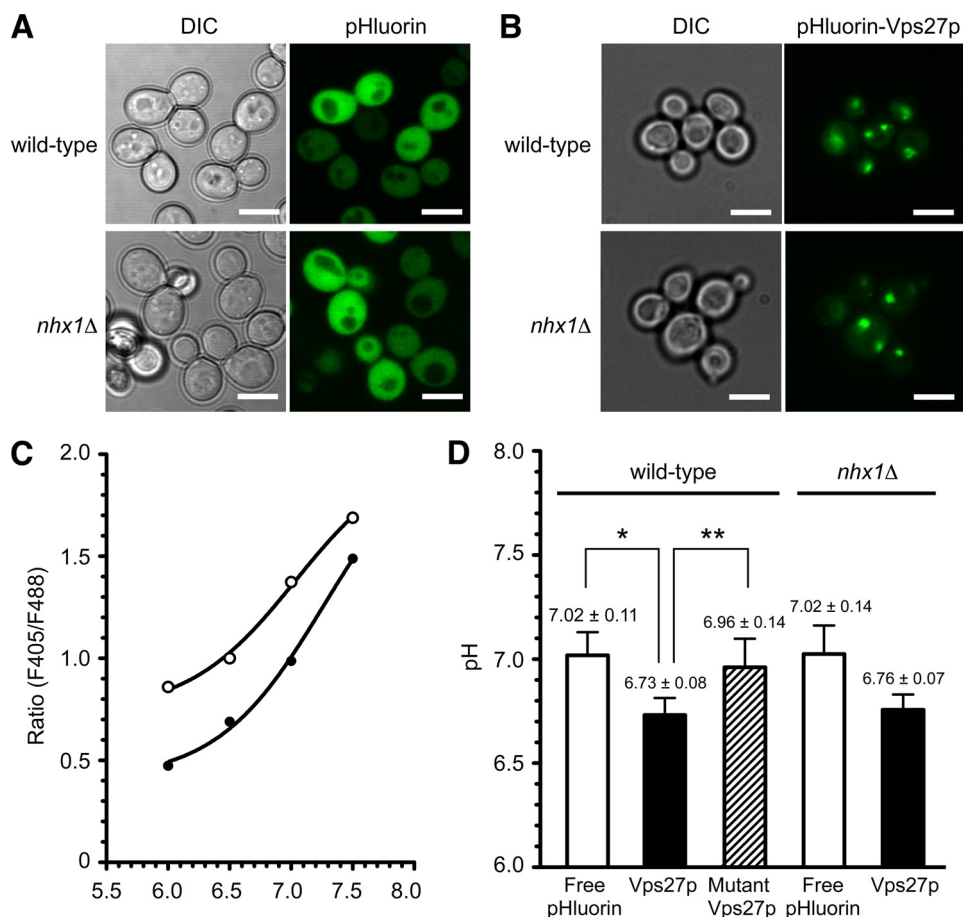


FIGURE 8. The cytoplasmic surface pH of endosomes is acidified compared with the bulk cytoplasmic space. *A* and *B*, shown is intracellular localization of free pHluorin (*A*) and pHluorin-Vps27p (*B*) in wild-type and *nhx1Δ* cells. Wild-type (BY4742) and *nhx1Δ* (MKY0804) cells transformed with pRS316GAP1p-pHluorin or pRS316GAP1p-pHluorin-VPS27 were grown to the logarithmic phase in APG medium (pH 5.5) at 30 °C and observed with a fluorescence microscope. Scale bars, 5 μ m. *C*, representative pH standard curves for free pHluorin and pHluorin-Vps27p are shown. Cells expressing free pHluorin (closed circles) or pHluorin-Vps27p (open circles) were grown to logarithmic phase in APG medium (pH 5.5) at 30 °C and then incubated in pH calibration buffer preadjusted to the indicated pH. The cells were sequentially excited with 405- and 488-nm lasers, and fluorescence images for pHluorin were obtained with a laser confocal microscope and the ratios (fluorescence intensity 405/488 nm) plotted. *D*, a comparison of bulk cytoplasmic pH (for free pHluorin) and endosomal surface pH (for pHluorin-Vps27p) is shown. Wild-type (BY4742) or *nhx1Δ* (MKY0804) cells transformed with pRS316GAP1p-pHluorin, pRS316GAP1p-pHluorin-VPS27, or pRS316GAP1p-pHluorin-VPS27-H190A/H191A were grown to logarithmic phase in APG medium (pH 5.5) at 30 °C and fixed on glass bottom dishes coated with concanavalin A. The cells were sequentially excited with 405- and 488-nm lasers, and fluorescence images for pHluorin were obtained with a laser confocal microscope. pH values were calculated from the ratios (fluorescence intensity 405/488 nm). White bar, free pHluorin; black bar, pHluorin-Vps27p; hatched bar, pHluorin-Vps27p-H190A/H191A. Data are the means \pm S.D. of at least three independent experiments. *, $p < 0.005$; **, $p < 0.05$.

observation does not appear to be consistent with our current proposal. However, because a change in Vps27p distribution or *in vitro* MVB formation comparable with that seen in *nhx1Δ* cells was observed after even a small shift (<0.5) in the intracellular pH (Figs. 6 and 7), the actual difference in endosomal surface pH between wild-type and *nhx1Δ* cells might be much smaller than could be measured in our system. Such tight pH regulation may be required for proper Vps27p recruitment. In addition, it should be noted that in *nhx1Δ* cells, most of the overexpressed pHluorin-Vps27p appeared to be localized to the endosomes (Fig. 8*B*). This is different from our observation that approximately half of the Vps27p was distributed diffusely through the cytoplasm when it was expressed at the endogenous level in *nhx1Δ* cells (Fig. 5, *A–C*). This accumulation of GFP-Vps27p after the loss of Nhx1p might affect detection of the surface pH, concealing differences between the surface pH of wild-type and *nhx1Δ* cells. The cause of the endosomal accumulation of overexpressed pHluorin-Vps27p remains unclear at present. It is known that ESCRTs shuttle between the endo-

somal membrane and the cytoplasm (3, 48). Although ESCRT-III is dissociated from endosomal membrane by Vps4p (14), the dissociation of the ESCRT-0/I/II complexes might require additional unknown factors (3, 48). One possible explanation for the endosomal accumulation of Vps27p in *nhx1Δ* cells is that an additional factor is involved in dissociation of Vps27p (ESCRT-0) from endosomal membranes. This putative factor might not function sufficiently in the absence of Nhx1p.

We could not rule out completely the possibility that a change in the luminal pH in *nhx1Δ* cells affects Vps27p recruitment. Luminal acidification might cause a dynamic change in lipid composition of the endosomal membrane, especially a potential reduction in PI(3)P, leading to defective Vps27p recruitment to the endosome.

It has been suggested that phospholipid lysobisphosphatidic acid, which is enriched in the MVBs of mammalian cells, promotes the formation of internal vesicles in liposomes *in vitro* and that vesicle formation depends on acidification of the

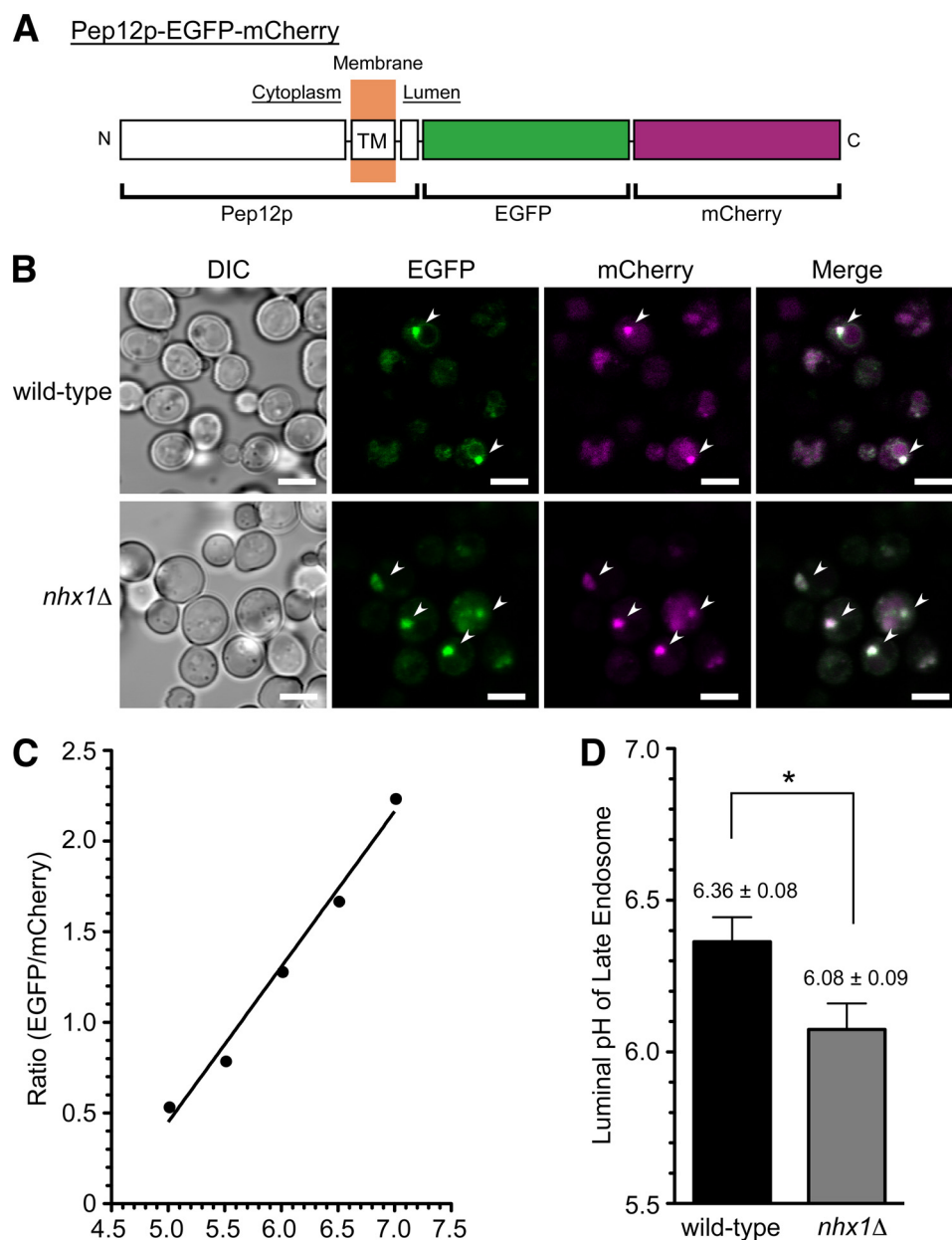


FIGURE 9. Loss of Nhx1p causes acidification of the endosomal lumen. *A*, shown is a schematic illustration of the chimeric protein used as a late endosome-targeted pH probe. EGFP (pH-sensitive) and mCherry (pH-insensitive) were fused to the C terminus of the late endosome-localized t-SNARE protein, Pep12p. TM, transmembrane. *B*, wild-type (BY4742) and *nhx1Δ* (MKY0804) cells transformed with pRS316GAP1p-PEP12-EGFP-mCherry were grown to logarithmic phase in APG medium (pH 5.5) at 30 °C and then fixed on glass-bottom dishes coated with concanavalin A. Fluorescence images of EGFP (green) and mCherry (magenta) were obtained with a laser scanning confocal microscope. Scale bars, 5 μm. *C*, representative pH standard curve for the endosomal pH probe. Yeast cells expressing Pep12p-EGFP-mCherry were grown to logarithmic phase in APG medium (pH 5.5) at 30 °C and then incubated in pH calibration buffer preadjusted to the indicated pH. Fluorescence intensities of EGFP and mCherry were measured with a laser confocal microscope, and the ratios (EGFP/mCherry) are plotted. *D*, wild-type (BY4742) or *nhx1Δ* (MKY0804) cells transformed with pRS316GAP1p-PEP12-EGFP-mCherry were grown to logarithmic phase in APG medium (pH 5.5) at 30 °C and fixed on glass-bottom dishes coated with concanavalin A. The fluorescence intensities of EGFP and mCherry were obtained with a laser confocal microscope, and the luminal pH of the endosome was calculated from the ratio of fluorescence intensities (EGFP/mCherry). Data are presented as the means ± S.D. of at least four independent experiments. *, $p < 0.005$.

lumen of the liposome (49). However, there is no evidence for the presence of lysobisphosphatidic acid in yeast cells, and no Vps proteins have emerged as possible regulators of lysobisphosphatidic acid levels. We also observed GFP-Cps1p localization in *vma2Δ* cells lacking Vma2p, an essential V_1 subunit of V-ATPase. The loss of V-ATPase function had no detectable effect on the vacuolar localization of GFP-Cps1p in our experiments.⁴ However, in *vma2Δ nhx1Δ* cells, the mislocalization of GFP-Cps1p was identical to that of *nhx1Δ* cells.⁴ Because the organ-

ellar lumen is maintained at an acidic pH by alternative mechanisms, even in *vma2Δ* cells lacking V-ATPase activity (50, 51), our data provide no evidence for the requirement of an acidic endosomal lumen in MVB formation. However, this result suggests that Nhx1p can function independently of V-ATPase activity, at least in MVB formation, which is consistent with the results of carboxypeptidase Y secretion in *vma2Δ* or *nhx1Δ* cells, as reported previously (30). Furthermore, this finding supports the idea that Nhx1p contributes to MVB formation by

regulating the surface pH rather than the luminal pH of endosomes.

Our results suggest for the first time that the pH of the cytoplasmic surface of endosomes is involved in the control of endosomal functions, such as MVB formation. This finding reveals the unsuspected implication of a role for ion transporters in endosomal function. The precise mechanism underlying control of the Vps27p-PI(3)P interaction by Nhx1p and the contribution of local surface pH to other endocytic processes will be the focus of future studies.

Acknowledgments—We thank Dr. James E. Rothman (Yale University School of Medicine) for providing the expression plasmid encoding pHluorin. We also thank Dr. Dick Hoekstra (University Medical Center of Groningen) and Dr. Ryuichi Ohgaki (Osaka University, School of Medicine) for extensive review of the manuscript.

REFERENCES

- Lee, J. A., Beigneux, A., Ahmad, S. T., Young, S. G., and Gao, F. B. (2007) *Curr. Biol.* **17**, 1561–1567
- Katzmann, D. J., Odorizzi, G., and Emr, S. D. (2002) *Nat. Rev. Mol. Cell Biol.* **3**, 893–905
- Raiborg, C., and Stenmark, H. (2009) *Nature* **458**, 445–452
- Filimonenko, M., Stuffers, S., Raiborg, C., Yamamoto, A., Malerød, L., Fisher, E. M., Isaacs, A., Brech, A., Stenmark, H., and Simonsen, A. (2007) *J. Cell Biol.* **179**, 485–500
- Carlton, J. G., and Martin-Serrano, J. (2007) *Science* **316**, 1908–1912
- Kleijmeer, M., Ramm, G., Schuurhuis, D., Griffith, J., Rescigno, M., Ricciardi-Castagnoli, P., Rudensky, A. Y., Ossendorp, F., Melief, C. J., Stoorvogel, W., and Geuze, H. J. (2001) *J. Cell Biol.* **155**, 53–63
- Bankaitis, V. A., Johnson, L. M., and Emr, S. D. (1986) *Proc. Natl. Acad. Sci. U.S.A.* **83**, 9075–9079
- Rothman, J. H., and Stevens, T. H. (1986) *Cell* **47**, 1041–1051
- Raymond, C. K., Howald-Stevenson, I., Vater, C. A., and Stevens, T. H. (1992) *Mol. Biol. Cell* **3**, 1389–1402
- Katzmann, D. J., Stefan, C. J., Babst, M., and Emr, S. D. (2003) *J. Cell Biol.* **162**, 413–423
- Wollert, T., Wunder, C., Lippincott-Schwartz, J., and Hurley, J. H. (2009) *Nature* **458**, 172–177
- Wollert, T., and Hurley, J. H. (2010) *Nature* **464**, 864–869
- Hurley, J. H., and Hanson, P. I. (2010) *Nat. Rev. Mol. Cell Biol.* **11**, 556–566
- Katzmann, D. J., Babst, M., and Emr, S. D. (2001) *Cell* **106**, 145–155
- Rieder, S. E., Banta, L. M., Köhrer, K., McCaffery, J. M., and Emr, S. D. (1996) *Mol. Biol. Cell* **7**, 985–999
- Brett, C. L., Donowitz, M., and Rao, R. (2005) *Am. J. Physiol. Cell Physiol.* **288**, C223–C239
- Sardet, C., Franchi, A., and Pouyssegur, J. (1989) *Cell* **56**, 271–280
- Orlowski, J., Kandasamy, R. A., and Shull, G. E. (1992) *J. Biol. Chem.* **267**, 9331–9339
- Tse, C. M., Levine, S. A., Yun, C. H., Montrose, M. H., Little, P. J., Pouyssegur, J., and Donowitz, M. (1993) *J. Biol. Chem.* **268**, 11917–11924
- Attaphitaya, S., Park, K., and Melvin, J. E. (1999) *J. Biol. Chem.* **274**, 4383–4388
- Baird, N. R., Orlowski, J., Szabó, E. Z., Zaun, H. C., Schultheis, P. J., Menon, A. G., and Shull, G. E. (1999) *J. Biol. Chem.* **274**, 4377–4382
- Numata, M., and Orlowski, J. (2001) *J. Biol. Chem.* **276**, 17387–17394
- Fukura, N., Ohgaki, R., Matsushita, M., Nakamura, N., Mitsui, K., and Kanazawa, H. (2010) *J. Membr. Biol.* **234**, 149–158
- Ohgaki, R., Matsushita, M., Kanazawa, H., Ogihara, S., Hoekstra, D., and van Ijzendoorn, S. C. D. (2010) *Mol. Biol. Cell* **21**, 1293–1304
- Nakamura, N., Tanaka, S., Teko, Y., Mitsui, K., and Kanazawa, H. (2005) *J. Biol. Chem.* **280**, 1561–1572
- Ohgaki, R., van Ijzendoorn, S. C., Matsushita, M., Hoekstra, D., and Kanazawa, H. (2011) *Biochemistry* **50**, 443–450
- Nass, R., and Rao, R. (1998) *J. Biol. Chem.* **273**, 21054–21060
- Mitsui, K., Matsushita, M., and Kanazawa, H. (2010) *Biochem. J.* **432**, 343–352
- Brett, C. L., Tukaye, D. N., Mukherjee, S., and Rao, R. J. (2005) *Mol. Biol. Cell* **16**, 1396–1405
- Bowers, K., Levi, B. P., Patel, F. I., and Stevens, T. H. (2000) *Mol. Biol. Cell* **11**, 4277–4294
- Brachmann, C. B., Davies, A., Cost, G. J., Caputo, E., Li, J., Hieter, P., and Boeke, J. D. (1998) *Yeast* **14**, 115–132
- Wallis, J. W., Chrebet, G., Brodsky, G., Rolfe, M., and Rothstein, R. (1989) *Cell* **58**, 409–419
- Sherman, F. (2002) *Guide to Yeast Genetics and Molecular and Cell Biology, Part B*, pp 3–41, Academic Press Inc, San Diego, CA
- Nass, R., Cunningham, K. W., and Rao, R. (1997) *J. Biol. Chem.* **272**, 26145–26152
- Kanazawa, H., Miki, T., Tamura, F., Yura, T., and Futai, M. (1979) *Proc. Natl. Acad. Sci. U.S.A.* **76**, 1126–1130
- Odorizzi, G., Babst, M., and Emr, S. D. (1998) *Cell* **95**, 847–858
- Vida, T. A., and Emr, S. D. (1995) *J. Cell Biol.* **128**, 779–792
- Nickerson, D. P., West, M., and Odorizzi, G. (2006) *J. Cell Biol.* **175**, 715–720
- Lee, S. A., Eyeson, R., Cheever, M. L., Geng, J., Verkhusha, V. V., Burd, C., Overduin, M., and Kutateladze, T. G. (2005) *Proc. Natl. Acad. Sci. U.S.A.* **102**, 13052–13057
- He, J., Vora, M., Haney, R. M., Filonov, G. S., Musselman, C. A., Burd, C. G., Kutateladze, A. G., Verkhusha, V. V., Stahelin, R. V., and Kutateladze, T. G. (2009) *Proteins Struct. Funct. Genet.* **76**, 852–860
- Ungermann, C., Wickner, W., and Xu, Z. Y. (1999) *Proc. Natl. Acad. Sci. U.S.A.* **96**, 11194–11199
- Maranda, B., Brown, D., Bourgoin, S., Casanova, J. E., Vinay, P., Ausiello, D. A., and Marshansky, V. (2001) *J. Biol. Chem.* **276**, 18540–18550
- Aniento, F., Gu, F., Parton, R. G., and Gruenberg, J. (1996) *J. Cell Biol.* **133**, 29–41
- Gu, F., and Gruenberg, J. (2000) *J. Biol. Chem.* **275**, 8154–8160
- Bianchini, L., and Pouyssegur, J. (1994) *J. Exp. Biol.* **196**, 337–345
- Steinberg, B. E., Huynh, K. K., Brodovitch, A., Jabs, S., Stauber, T., Jentsch, T. J., and Grinstein, S. (2010) *J. Cell Biol.* **189**, 1171–1186
- Scott, C. C., and Gruenberg, J. (2011) *Bioessays* **33**, 103–110
- Nickerson, D. P., Russell, M. R., and Odorizzi, G. (2007) *EMBO Rep.* **8**, 644–650
- Matsuo, H., Chevallier, J., Mayran, N., Le Blanc, I., Ferguson, C., Fauré, J., Blanc, N. S., Matile, S., Dubochet, J., Sadoul, R., Parton, R. G., Vilbois, F., and Gruenberg, J. (2004) *Science* **303**, 531–534
- Nelson, H., and Nelson, N. (1990) *Proc. Natl. Acad. Sci. U.S.A.* **87**, 3503–3507
- Nelson, N., Perzov, N., Cohen, A., Hagai, K., Padler, V., and Nelson, H. (2000) *J. Exp. Biol.* **203**, 89–95